Eur. Phys. J. A **27**, 59–65 (2006)
DOI 10.1140/epja/i2005-10195-x

THE EUROPEAN PHYSICAL JOURNAL A

Measurements of isomeric cross-section ratios for neutron capture in the resonances region

X. Ledoux[1,a], J. Sigaud[1], T. Granier[1], J-P. Lochard[1], Y. Patin[1], P. Pras[1], C. Varignon[1], J-M. Laborie[2], Y. Boulin[2], and F. Gunsing[3]

[1] CEA/DIF/DPTA Service de Physique Nucléaire, BP 12, F-91680 Bruyères-le-Châtel, France
[2] CEA/DIF/DASE Service de Radioanalyse, Chimie et Environnement, BP 12, F-91680 Bruyères-le-Châtel, France
[3] CEA/DSM/DAPNIA/SPhN CEA-Saclay, F-91191 Gif-sur-Yvette Cedex, France

Received: 7 July 2005 / Revised version: 10 January 2006 /
Published online: 3 February 2006 –
Communicated by C. Signorini

Abstract. The creation of isomeric nuclei by neutron capture in the resonances energy range was studied with the lead slowing-down assembly CIRENE. The isomeric-ratio measurement of 8 nuclei allows to determine the spin of the compound nucleus at the binding energy. An experiment on ^{177}Lu underlines the role of the spin of a resonance on the isomeric-state feeding probability.

PACS. 23.20.Lv γ transitions and level energies – 24.60.Dr Statistical compound-nucleus reactions – 25.40.Ny Resonance reactions – 29.30.Kv X- and γ-ray spectroscopy

1 Introduction

In numerous cases, the compound nucleus following a nuclear interaction decays by gamma emission to either an isomeric or the ground state. The relative feeding probability of these two states depends strongly on the spins of the compound nucleus, the isomeric and ground states [1]. It cannot be predicted by theoretical calculations because of the generally very complex decay paths and in part because the compound nucleus spin is unknown. We propose an original method to determine experimentally the feeding ratio between isomer and ground state in case where the compound nucleus spin is known (after resonance neutron capture). The isomeric ratio, defined by IR $= \sigma^m/(\sigma^m + \sigma^g)$, is the relevant observable for at least two reasons. The compound nucleus formation cross-section is independent of the following de-excitation and a cross-section ratio is easier to measure than an absolute cross-section. IR has been measured for several decades through several production reactions like (p,n), (d,p), (d,2n), (d,4n),(p,3n), (α,n), (^{3}He,n), (γ,n), (n,2n), (n,α) or (n,γ) [1–7]. Capture reactions are generally studied at thermal energy except by Bishop *et al.* [4] who measured IR in an epithermal neutron flux.

In this case only *s*-wave neutrons are captured leading to a compound nucleus spin of $J \pm 1/2$ where J is the spin of the target nucleus. Huizenga and Vandenbosch [1] made some calculations to reproduce the measured IR at thermal energy and predict the value at the resonance energy (not measured). They concluded that the spin gap between the compound nucleus and the isomeric and fundamental states is a dominant parameter on the isomeric feeding. We propose to confirm this trend by measuring the IR following the neutron capture at resonance energy which presents the advantage of forming a compound nuclear state of defined spin. In addition, the differences of IR at a resonance energy and in thermal neutron flux allows to determine the spin of the compound nuclear state at thermal energy.

Most of the nuclei with large A present capture cross-section resonances in the 0.1 eV–10 keV range which can reach several tenth of thousands of barns. A huge gain in capture rate can be envisaged by capture in a resonance in comparison to capture at thermal energy which is usually quite small. In addition the spin of the compound nucleus following a resonant capture could favor isomeric-state feeding. The aim of this work is to measure the IR at the capture resonance energy and to compare it with the values at thermal energy.

The lead slowing-down assembly CIRENE (Création d'Isomères dans les Résonances NEutroniques) was built for this study. This kind of set-up allows to reach high-intensity neutron flux in the 0.1 eV–10 keV range [8–11]. In such a neutron flux the main part of the captures (up to 90% depending on the nucleus) takes place in the single large low-energy resonance. The spin of the compound nucleus following the capture is thus well determined.

[a] e-mail: xavier.ledoux@cea.fr

The IRs of several nuclei have been measured at the energy of the main resonance. The first part of this paper describes the lead pile CIRENE. The measurements of the isomeric ratios are then exposed and discussed. Finally, an original experiment dedicated to the IR measurement on two tagged resonances of ^{177}Lu is presented.

2 Experimental set-up

2.1 Principle

Slowing-down spectrometers have been employed since the 50's [8] for various applications such as cross-section measurements [9–11] or radioactive waste transmutation studies [12–14]. The average relative energy lost by a neutron in elastic scattering with a nucleus of mass A is given by eq. (1):

$$\frac{\langle \Delta E \rangle}{E} = \frac{2A}{(A+1)^2}\,. \qquad (1)$$

For a heavy nucleus, like lead ($A \simeq 207$), the neutron looses 1% of its energy each time it scatters. The average energy loss being smaller than the resonance width, this adiabatic slowing-down process allows to describe a narrow resonance with a high capture probability (see introduction). Due to its high mass number and an elastic cross-section more than 4 orders of magnitude greater than the capture one in the 0.1 eV–10 keV range, lead is the best candidate for such an application. Neutrons of a few MeV produced in the centre of a large lead pile slow down by inelastic (above 0.57 MeV) and elastic scattering until thermal energy. This kind of set-up leads to a high neutron flux in the 0.1 eV–10 keV range (as compared to most time-of-fligth neutron sources) which is precisely the domain of resonant cross-sections for most medium- and heavy-mass nuclei.

The neutron flux in such an assembly has been simulated using the MCNP [15] neutron transport code. The use of the neutron capture cross-sections from the ENDF/B-VI [16] data file allows to calculate the number of the captures as a function of the neutron energy. In the case of ^{186}W (fig. 1) 89% of the total number of captures takes place in the first large low-energy resonance at 18.8 eV.

The spectrometer operation mode, using the correlation between the slowing-down time and the neutron kinetic energy [14], was investigated for another study [17]. For this work only continuous beam is considered and the lead pile is used as an irradiation tool.

2.2 Lead pile

Calculations performed with the MCNP [15] code show that the flux (normalized per source neutron) in the energy region of interest depends on the size of the lead cube. The optimal size leads to a 380 t lead assembly. Such a set-up being too heavy and too expensive a smaller cube

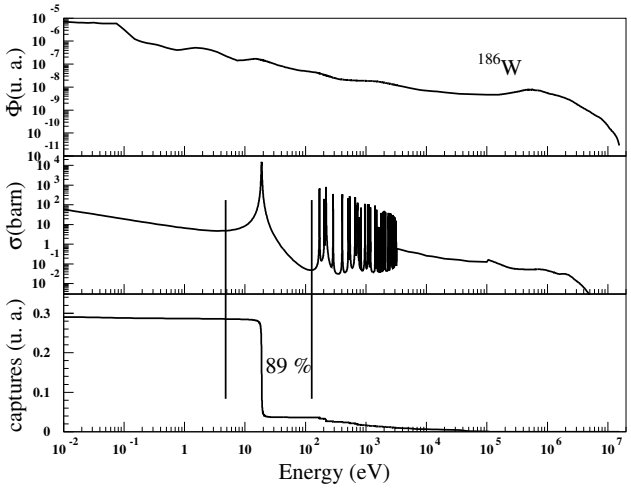

Fig. 1. Neutron flux inside CIRENE (top), capture cross-section of ^{186}W (middle) and number of captures integrated from E_{max} to E (bottom).

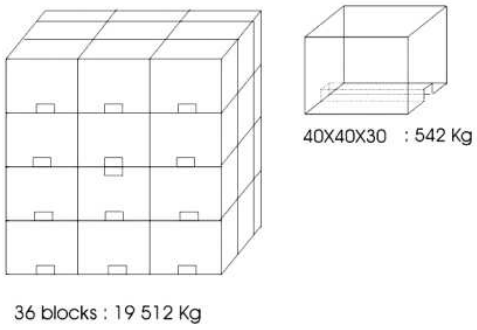

Fig. 2. The lead pile and one of the 36 elementary cubes. The channel allowing manipulation and samples introduction is clearly visible.

($L = 1.2\,\mathrm{m}$) was assembled. It is composed of 36 elementary cubes ($40 \times 40 \times 30\,\mathrm{cm}^3$) weighting 542 kg each (see fig. 2). A dedicated platform was built to support the lead pile and centre it at the beam line height. A rectangular channel, with a section of 10×5 cm^2, allows to move it, to insert samples in specific lead bricks and to insert the beam pipe inside the lead pile. Specific arrangement of the cubes offers the possibility to place the samples almost everywhere in the assembly.

Special attention was paid to the choice of the chemical lead purity. Neutron transport calculations performed with MCNP show that a few per cent of impurity can dramatically decrease the neutron flux. For example, 4% of antimony (usually mixed in lead for mechanical reasons), reduces neutron flux by a factor of 100 in the 0.1 eV–10 keV range.

2.3 Neutron source

The neutrons were produced by the (12 MeV) d + Be reaction. A 15 μA deuterons beam impinging on a 1 mm thick target produces several 10^{11} neutrons per second in 4π. The beryllium target, located at the end of the pipe, is placed at the centre of the lead cube. A specific target was designed in order to address several technical constraints like heat evacuation and reduced activation risks. A liquid cooling system was necessary to evacuate the 180 watts deposited in the beryllium disk. Considering machining difficulties, aluminum was the best-suited metal for the target support. Its heat capacity, close to that of beryllium, makes the cooling easier. In addition only short-lived activation elements are produced in aluminum by fast and thermal neutron fluxes. The most abundant isotope ^{24}Na, produced by the Al(n,α) reaction, has a relatively short half-life ($T_{1/2} = 14.92$ h). Therefore the set-up is accessible for handling after only a few days of decay.

2.4 Samples and detectors

The sample thickness is determined by the capture cross-section in the main resonance (σ). The condition $N\sigma = 1/100$ (with N the number of atoms per cm^2) ensures not to disturb the neutron flux reducing the self-shielding effect to negligible level. Taking into account the density and the isotopic abundance it corresponds to thicknesses of 0.06 and 0.36 μm for gold and silver, respectively. Thus samples are small discs of lead (18 mm in diameter and 1 mm thick) on which the studied isotope is evaporated. The backing is composed of high-purity lead (99.95%) in order to reduce the activation of impurities which could pollute the gamma-ray spectra. The samples are placed inside dedicated lead bricks ($20 \times 10 \times 5$ cm^3) with special holes. The bricks can then be put almost everywhere in the pile using the channels mentioned in sect. 2.2.

All the studied nuclei, in ground and isomeric state, are radioactive (see details in sect. 3.1) and can be detected by gamma spectroscopy. A 90% HPGe coaxial detector was used with a classical spectroscopic chain composed of pre-amplifier, amplifier and multichannel analyzer. Almost two minutes were necessary to enter in the experimental room, extract the sample out of the cube and put it in front of the detector placed outside. For this reason, no element with a half-life shorter than that of ^{110m}Ag ($T_{1/2} = 24.6$ s) could be studied. A shielding composed of 10 cm thick lead (to reduce the background due to the gamma rays coming from concrete) surrounding 1 cm copper (to stop X-rays generated in the lead shielding) surrounded the germanium detector. Therefore a low radioactivity level (in case of long-lived isomer) could be measured. The germanium detection efficiency has been determined using calibrated sources on the overall spectra from 59 keV to 1332 keV.

2.5 Neutron flux determination

The neutron flux is determined by calculations and by irradiation. A precise geometrical description of the set-up including the beam pipe, the target and the lead cube is used in the neutron transport code MCNP. The neutron source energy spectra and angular distribution are generated according to the data published by Brede *et al.* [19]. The neutron flux is then calculated at the positions of the samples. The inclusion of the capture cross-section allows to evaluate the reaction rate in the sample (see fig. 1). The self-attenuation is negligible because of the small thickness of the sample (see sect. 2.4).

These calculations are compared to the irradiation of gold and tungsten samples. These elements are very well adapted because of their huge capture cross-sections in the resonances and the half-lives of ^{198}Au and ^{187}W (see table 1). A good agreement has been found between the number of source neutrons obtained from the simulations and deduced from the irradiation of gold and silver samples placed at numerous positions. Thus a 12 MeV deuteron beam with an intensity of 15 μA produces $2 \cdot 10^{11}$ neutrons source per second. A relative flux monitoring is performed in line using a small ^{3}He detector placed inside the lead pile.

This beam intensity corresponds to a flux of 10^8 n cm^{-2} s^{-1} in the 0.1 eV–10 keV range. The irradiation time was determined by the period of the studied elements.

Table 1. ^{197}Au and ^{186}W characteristics [16,18].

Element	Resonance energy	Cross-section	$T_{1/2}$ of nucleus $(A+1)$
^{197}Au	4.906 eV	27400 b	2.69 d
^{186}W	18.83 eV	15000 b	23.72 h

3 Isomeric-state studies

3.1 Isomeric choice criteria

The choice of the studied nucleus depends on several criteria:

1. A resonance with a large neutron capture cross-section.
2. An unstable ground state in order to detect isomer and ground state by gamma-ray spectroscopy. The chosen nuclei decay by β emission followed by gamma rays emitted by the daughter nuclei.
3. Isomer and ground-state periods are limiting factors. Short periods are limited to around 1/2 minute (see sect. 2.4). The long periods are limited by the detection level.
4. The element should be isotopically abundant and not toxic in order to be evaporated.

Finally, the isomeric ratios of 8 nuclei, whose characteristics are given in table 2, have been measured.

3.2 Isomeric-ratios measurement

Let us consider a nucleus X which leads by neutron capture to the nucleus Z_g in the ground state with a cross-

Table 2. Half-life of ground and isomeric states, energy, isomeric transition probability and neutron binding energy of the 8 studied nuclei [20].

Compound nucleus	T_g	T_m	E (keV)	p (%)	S_n (keV)
^{110}Ag	24.6(2) s	249.79(20) d	117.59	1.36(6)	6809.2(1)
^{122}Sb	2.7238(2) d	4.191(3) min	163.5591(17)	100	6806.9(10)
^{134}Cs	2.0648(10) y	2.903(8) h	138.7441(26)	100	6891.54(1)
^{152m_1}Eu	13.537(6) y	9.3116(13) h	45.5998(4)	0	6306.72(10)
^{152m_2}Eu	13.537(6) y	96(1) min	147.86(10)	100	6306.72(10)
^{154}Eu	8.593(4) y	46.3(4) min	145.3(3)	100	6442.0(3)
^{188}Re	17.005(4) h	18.6(1) min	172.069(9)	100	5871.6(3)
^{177}Lu	6.734(12) d	160.4(3) d	970.1749(25)	21.7(6)	7072.2(6)

section σ_g and a decay constant λ_g and to nucleus Z_m in the isomeric state with a cross-section σ_m and a decay constant λ_m. During an irradiation period t_i of a sample containing N nuclei exposed to a neutron flux ϕ, the number of metastable N_m and ground-state N_g nuclides are

$$N_m(t) = \frac{R\sigma_m}{\lambda_m}(1 - e^{-\lambda_m t}), \tag{2}$$

$$N_g(t) = R\left[\left(\frac{\sigma_g + p\sigma_m}{\lambda_g}\right) + \left(\frac{\sigma_g\lambda_m + p\sigma_m\lambda_m - \sigma_g\lambda_g}{\lambda_g(\lambda_g - \lambda_m)}\right)e^{-\lambda_g t} - \frac{p\sigma_m}{(\lambda_g - \lambda_m)}e^{-\lambda_m t}\right], \tag{3}$$

where p is the transition probability from isomer to ground state (see column 5 of table 2) and $R = \phi N$. The cross-section ratio can be deduced from eqs. (2) and (3):

$$\frac{\sigma_g}{\sigma_m} = \frac{1 - e^{-\lambda_m t_i}}{1 - e^{-\lambda_g t_i}}\left[\frac{\lambda_g N_g(t_i)}{\lambda_m N_m(t_i)} - \frac{p\lambda_g}{\lambda_g - \lambda_m}\right] + \frac{p\lambda_m}{\lambda_g - \lambda_m}. \tag{4}$$

After a decay time t_r the sample is placed in front of a germanium detector during t_m. The peak area of the detected gamma emitted by Z_m and Z_g with branching ratio I_m and I_g are

$$S_m = \epsilon_m I_m N_m(t_i) h_m(t), \tag{5}$$

$$S_g = \epsilon_g I_g\left[N_g(t_i)h_g(t) + \frac{p\lambda_m}{\lambda_g - \lambda_m}N_m(t_i)h_m(t) - \frac{p\lambda_m}{\lambda_g - \lambda_m}N_m(t_i)h_g(t)\right], \tag{6}$$

where ϵ_m and ϵ_g are the detection efficiencies for isomeric- and ground-state gamma, respectively, and h the time-dependent function $h_m(t) = e^{-\lambda_m t_r}(1 - e^{-\lambda_m t_m})$.

$N_m(t_i)$ is deduced from eq. (5). The ratio $\frac{N_g(t_i)}{N_m(t_i)}$ (needed in eq. (4)) is deduced from eqs. (5) and (6):

$$\frac{N_g(t_i)}{N_m(t_i)} = \frac{h_m(t)}{h_g(t)}\left[\frac{S_g\epsilon_m I_m}{S_m\epsilon_g I_g} - \frac{p\lambda_m}{\lambda_g - \lambda_m}\right] + \frac{p\lambda_m}{\lambda_g - \lambda_m}. \tag{7}$$

The cross-section ratio can now be calculated (eq. (4)) and the IR is

$$\mathrm{IR} = \frac{\sigma_m}{\sigma_g + \sigma_m} = \frac{1}{1 + \frac{\sigma_g}{\sigma_m}}. \tag{8}$$

A precise knowledge of sample thickness and absolute neutron flux is not necessary to determine IR because ϕ and N do not appear in eq. (4). Note that this result is the same than Belov *et al.* published in ref. [7] where calculations are not developed. In some cases, λ_m and λ_g being very different, the gamma measurements are performed after two different irradiation duration times.

3.3 Results

In order to suppress the thermal component, the samples are surrounded by 0.8 mm cadmium shielding. Calculations performed with the MCNP code and ENDF/B-VI evaluated data files show that for each of the studied nuclei more than 80% of the total number of captures take place in the lowest-energy resonance. The case of ^{186}W is presented in fig. 1.

The measured IR (written IR_{res} for resonance) and thermal IR (IR_{therm}) are presented in table 3. Uncertainties take into account statistical effects and incomplete gamma detection efficiency knowledge. The spins of ground and isomeric states are also printed. In two cases, ^{110}Ag and ^{122}Sb, IR_{res} is two times greater than IR_{therm}. For the other 5 nuclei we have $\mathrm{IR}_{res} \simeq \mathrm{IR}_{therm}$.

4 Case of ^{177}Lu

4.1 Neutron filter technique

The neutron capture cross-sections of ^{113}Cd and ^{176}Lu (see fig. 3) present very useful characteristics. Cadmium is well known to be very efficient in shielding against neutrons below 0.3 eV. The isotope ^{176}Lu has a main resonance at $E = 0.141$ eV with a spin $J = 13/2$ and a series of resonances in the 1–20 eV range which have almost all a spin $J = 15/2$.

In the CIRENE neutron flux, most of the captures on a ^{176}Lu sample occur in the resonance at $E = 0.141$ eV with a spin $J = 13/2$. When the same sample is surrounded by a cadmium shielding all the captures take place on the resonances at $E \geq 1$ eV with a spin $J = 15/2$. The irradiations with and without Cd allow to measure the IR of ^{177}Lu following a compound nucleus of tagged spin 13/2 and 15/2.

Table 3. Isomeric ratios with thermal neutrons, measured with CIRENE (columns 2 and 3) together with the spins of the target nucleus $A-1$, and the spins of the ground state, the isomeric state and the resonance state of the compound nucleus [18].

Compound nucleus	IR_{therm}	IR_{res}	$J_{(A-1)}$	J_g	J_{iso}	J_{res}
^{110}Ag	5.1 10^{-2}	**(10.3 ± 2.0)** 10^{-2}	$1/2^-$	1^+	6^+	1
^{122}Sb	9.9 10^{-3}	**(2.36 ± 0.15)** 10^{-2}	$5/2^+$	2^-	8^-	3
^{134}Cs	8.6 10^{-2}	(8.6 ± 1.3) 10^{-2}	$7/2^+$	4^+	8^-	3
^{152m_1}Eu	35.9 10^{-2}	(36.4 ± 3.7) 10^{-2}	$5/2^+$	3^-	0^-	3
^{152m_2}Eu	6.8 10^{-4}	(6.7 ± 1.0) 10^{-4}	$5/2^+$	3^-	8^-	3
^{154}Eu	–	(1.33 ± 0.16) 10^{-4}	$5/2^+$	3^-	8^-	3
^{188}Re	3.7 10^{-2}	(3.44 ± 0.31) 10^{-2}	$5/2^+$	1^-	6^-	3

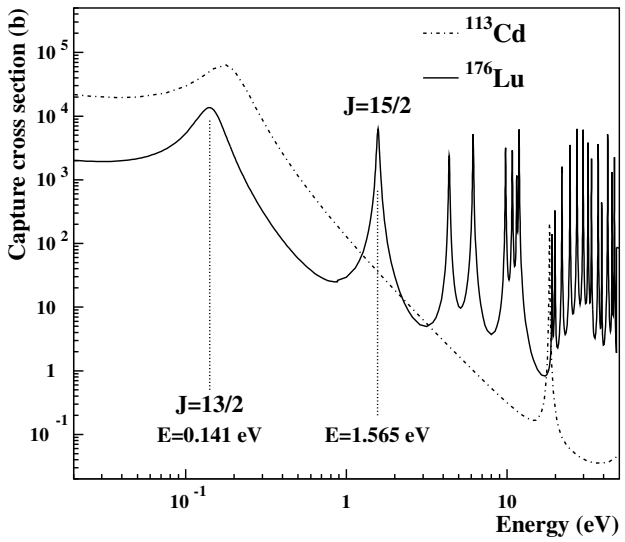

Fig. 3. Neutron capture cross-sections of ^{176}Lu and ^{113}Cd. The spin and energy of the two main resonances of ^{176}Lu are indicated.

Two 100 μg samples of 99.993% enriched ^{176}Lu (purified using the isotopic separator PARSIFAL [21] and put in carbon cylinders) have been irradiated at the same time in symmetric positions of the lead pile during 69 hours. The ^{177g}Lu ($T_{1/2}$ = 6.71 d) activity was measured a few days after the end of the irradiation. For the ^{177m}Lu ($T_{1/2}$ = 160.5 d) a decay period of several months was necessary to reach the total disappearance of ^{177g}Lu. The ^{176}Lu mass and the small isomer cross-section lead to very small ^{177m}Lu activity and required special analysis conditions described in the next section.

4.2 Isomeric lutetium activity measurement

In our samples the activity of ^{176}Lu ($T_{1/2} = 3.79\ 10^{10}$ y) is almost 20 times larger than that of ^{177m}Lu and the planar geometry was found to be the best suited to measure the ^{177m}Lu activity. For this particular measurement we used a low-background planar HPGe detector (area 23 cm^2, 2 cm thick). The detector was shielded with electrolytic copper and lead (12 cm low and 3 cm very low activity). Furthermore, the detector was set-up inside the deep underground laboratory of Modane [22,23], at the Italian-French border, under 1700 m rock (equivalent to 4400 m of water). In these conditions, the background between 10 and 400 keV was only 9 counts per hour.

Each sample was measured during ten days, and the activity was deduced from the two main lines emitted along with the decay of ^{177m}Lu at 208 and 228 keV. As the samples were measured very close to the detector, counting losses due to coincidence-summing effects affected the peak areas. The correction factors were calculated to be 1.43 and 1.54 for the peaks at 208 and 228 keV, respectively [24,25]. With the Gespecor software [26,27], we found correction factors of 1.57, 1.54 and 1.59 for the peaks at 88, 201 and 306 keV of ^{176}Lu.

Finally, the activity of ^{177m}Lu at the date of irradiation end, was found to be (11.9±1.8) 10^{-3} Bq, in the sample shielded by the Cd lining, and (13.8±2.1) 10^{-3} Bq, in the other sample. The activity uncertainty of ^{177m}Lu was evaluated to 15% (67% C.L.) by taking into account the statistical uncertainty, the uncertainty of the coincidence-summing correction factors, and the uncertainty of the detection efficiency.

4.3 Results

The results are presented in table 4. The statistical and systematic uncertainties are taken into account. As mentioned in sect. 3.2 the mass differences between the two lutetium samples (less than 12% according to the ^{176}Lu activity measurements) do not affect the IR measurement. It has been checked that the flux attenuation in the lutetium samples was negligible.

The ^{176}Lu(n,γ)^{177m}Lu and ^{176}Lu(n,γ)^{177g}Lu cross-sections reactions are well known for thermal neutrons. The respective values of 2.80 ± 0.17 b [28] and 2087.2 ± 70 b [18] leads to IR = (13.4 ± 1.0) 10^{-4}. The spin difference between the isomer ($J = 23/2^-$) and the ground

Table 4. ^{177}Lu Isomeric ratios for thermal neutrons [18], measured in this work without and with cadmium.

	Thermal flux	Without Cd	With Cd
IR	(13.4 ± 1.0) 10^{-4}	(10.6 ± 1.7) 10^{-4}	(28.1 ± 3.7) 10^{-4}

state ($J = 7/2^+$) probably explains this cross-section difference.

This work (see table 4) shows that the IR measured without cadmium is similar to the thermal one. In this case a large part of the captures takes place in the main resonance at 0.141 eV. When the capture occurs in the resonance at 1.565 eV and above a gain of a factor 2.5 is observed.

5 Discussion

These IR measurements give very interesting information about the compound nucleus spin and isomeric-feeding probabilities. In the Lu case the fact that the IR reached from a compound nucleus of spin 15/2 is 2.5 times higher than from a spin 13/2 shows that the spin gap between compound nucleus and isomeric state ($J = 23/2$ for the ^{177m}Lu) is a predominant parameter in the feeding probability.

The gain of IR_{res} in comparison to the IR_{therm} observed for ^{110}Ag, and ^{122}Sb can be explained as well. In the resonance energy range ($E < 1\,\mathrm{keV}$) neutrons being s-waves, the compound nucleus spin can only take 2 values $J = J_g \pm 1/2$. For ^{110}Ag (respectively ^{122}Sb) the spin of compound nucleus is $J_{CN} = 0$ or 1 ($J_{CN} = 2$ or 3). The isomeric-state (whose spin is $J_m = 6$ ($J_m = 3$)) feeding is favored by the spin of the compound nucleus produced at the main resonance $J_{CN} = 1$ ($J_{CN} = 3$) instead of $J_{CN} = 0$ ($J_{CN} = 2$).

In addition the fact that $\mathrm{IR}_{therm} < \mathrm{IR}_{res}$ leads to think that the spin of the compound nucleus following a thermal neutron capture energy is different to the spin at the resonance. The spin at thermal energy capture could be $J_{CN} = 0$ for ^{110}Ag and $J_{CN} = 2$ for ^{122}Sb. In this last case it corresponds to the resonance at the negative energy $E = -12$ eV given in ref. [18].

For ^{152m_1}Eu, ^{152m_2}Eu, ^{154}Eu and ^{188}Re the resonance spin leads to $J_{CN} = J_{A-1} + 1/2$ and the relation $\mathrm{IR}_{res} \simeq \mathrm{IR}_{therm}$ allows to conclude that it is the same value with a capture of thermal neutron. The same remark can be done for ^{134}Cs with $J_{CN} = J_{A-1} - 1/2$. For ^{177}Lu, $\mathrm{IR}_{res} \simeq \mathrm{IR}_{therm}$ means that the compound nucleus spin after a thermal capture is the same as that at the resonance of 0.141 eV, *i.e.* $J_{CN} = J_{A-1} - 1/2 = 13/2$.

In order to investigate if the present results can be predicted by the statistical model, we performed Monte Carlo calculations of the decay of the compound nucleus. At the high excitation energies above the neutron binding energies, where neutron resonances are observed, for most medium- and heavy-mass nuclei the nuclear system is extremely complex and no nuclear model is capable of predicting the energy and other properties of these excited states. Due to extreme configuration mixing, the nucleus in this regime above the neutron threshold has a statistical behaviour. This is expressed by the fact that the matrix elements related to nuclear state transitions have a random character, governed by a Gaussian distribution with zero mean. This statistical model of the compound nucleus is referred to as the Gaussian Orthogonal Ensemble.

Table 5. Isomeric ratios, measured with thermal neutrons (column 2), in this work (column 3) and calculated with a statistical model code.

Nucleus	IR_{therm}	IR_{res}	IR_{calc}
^{110}Ag	$5.1\ 10^{-2}$	$\mathbf{(10.3 \pm 2.0)}\ 10^{-2}$	$3.1\ 10^{-3}$
^{122}Sb	$9.9\ 10^{-3}$	$\mathbf{(2.36 \pm 0.15)}\ 10^{-2}$	$2.4\ 10^{-4}$
^{134}Cs	$8.6\ 10^{-2}$	$(8.6 \pm 1.3)\ 10^{-2}$	$1.5\ 10^{-4}$
^{152m_1}Eu	$35.9\ 10^{-2}$	$(36.4 \pm 3.7)\ 10^{-2}$	$2.1\ 10^{-3}$
^{152m_2}Eu	$6.8\ 10^{-4}$	$(6.7 \pm 1.0)\ 10^{-4}$	$1.4\ 10^{-4}$
^{154}Eu	–	$(1.33 \pm 0.16)\ 10^{-4}$	$1.8\ 10^{-4}$
^{188}Re	$3.7\ 10^{-2}$	$(3.44 \pm 0.31)\ 10^{-2}$	$8.4\ 10^{-2}$

We used a modified version of the code DICEBOX [29] in order to calculate the populations of the ground state and the isomeric states. Above the critical energy, the excitation spectrum of the nucleus is generated using level density information and the level transition probabilities are calculated using photon strength functions including width fluctuations. For the critical energy a value was chosen corresponding to the region where the available information in the level scheme starts to become scarse. For most of the considered nuclei the critical energy is roughly situated at about one fifth of the neutron binding energy. We have used the back-shifted Fermi gas model for the level densities with parameters taken from the RIPL-2 library [30]. The gamma-ray strength functions for $E1$ transitions were based on Lorentzian shaped giant dipole resonances, one for spherical and two for deformed nuclei. We have used the experimental values if available, and theoretical otherwise, from RIPL-2. For the $M1$ and $E2$ gamma-ray transitions we have used the energy-independent single-particle model. The gamma decay process in this region is considered completely statistical. Below the critical energy, where in general the decay is not statistical anymore, the levels and transition probabilities were taken from the ENSDF library [31]. The ratio of these populations should correspond to the measured isomeric cross-section ratio IR if the decay can be described by the statistical model. As can be seen from table 5, the calculated ratios are in some cases lower than the measured ratios by more than one order of magnitude, so underestimating the population of the metastable states. Reasonable changes in the input parameters change slightly the calculated ratios but do not reproduce the measured ratios. The gamma-ray decay spectrum of the compound nucleus is characterized by many thousands of primary gamma transitions, summing up to the total radiation width. For many isotopes having a metastable state, such privileged transitions, carrying several tens of percents of the radiation width, are known [31]. We believe that the disagreement between the measured and calculated values could have two origins. Spin and parity of levels involved in the gamma cascade are sometimes unknown or even wrong in the databases. The spin- and parity-dependent nuclear level densities [32] have not been taken into account in these simulations.

6 Conclusion

The Isomeric Ratio of 8 nuclei has been measured at the resonance energy using the slowing-down assembly CIRENE. The originality of this production mode is to form the compound nucleus with a well-known spin in contrast to thermal neutron capture. The IRs measured on two tagged resonances of ^{176}Lu of spin $J = 13/2$ and $J = 15/2$ differ by more than a factor 2. This confirms that the spin of the compound nucleus is a predominant parameter in the isomer and ground-state feeding. The differences between the IR measured at thermal energy and in the resonance allow to determine the main spin component of the compound nucleus following the capture of a thermal neutron. For two nuclei, ^{110}Ag and ^{122}Sb the main spin component of the compound nucleus at thermal energy is probably different from the spin of the first large s-wave resonance. It appears from the measurements that the isomeric states are always more populated than expected from predictions from statistical model calculations. This non-statistical effect is ascribed to nuclear structure effects resulting in a predominant feeding of the isomeric states.

References

1. J.R. Huizenga, R. Vandenbosch, Phys. Rev. **120**, 1305 (1960).
2. R. Vandenbosch, J.R. Huizenga, Phys. Rev. **120**, 1313 (1960).
3. B. Keisch, Phys. Rev. **129**, 769 (1963).
4. C.T. Bishop, H.K. Vonach, J.R. Huizenga, Nucl. Phys. **60**, 241 (1964).
5. R. Vanska, R. Riepo, Nucl. Phys. **179**, 525 (1981).
6. S.M. Qaim, A. Mushtaq, Phys. Rev. C **38**, 645 (1988).
7. A.G. Belov *et al.*, Phys. At. Nucl. **60**, 1773 (1997).
8. A.A. Bergman *et al.*, *Spectromètre neutronique fonctionnant d'après le temps de ralentissement des neutrons dans le plomb, Compte-Rendu de la 1ere conférence internationale sur les applications pacifiques de l'énergie atomique*, Vol. **IV** (Genève, 1955).
9. J. Chou, H. Werle, J. Nucl. Energy, **27**, 811 (1973).
10. R.E. Slovacek *et al.*, Nucl. Sci. Eng. **62**, 455 (1977).
11. S. Yamamoto, Nucl. Sci. Eng. **126**, 201 (1997).
12. C. Rubbia *et al.*, *Fast Neutron Incineration in the energy amplifier as alternative to geologic storage: the case of Spain*, CERN-LHC-97-001-EET.
13. C. Rubbia, *Resonance enhanced neutron captures for element activation and waste transmutation*, CERN-LHC-97-004-EET.
14. H. Arnould *et al.*, Phys. Lett. B **458**, 167 (1999).
15. J.F. Briesmeister (Editor), *MCNP - A General Monte-Carlo N-Particle Transport Code*, Version 4B, LA-12625-M, Los Alamos National Laboratory, Los Alamos, New Mexico (1997).
16. R.F. Rose (Editor), *ENDF/B Summary Documentation*, BNL-NCS-17541, 4th edition (ENDF/B-VI) 1991.
17. T. Granier *et al.*, Nucl. Instrum. Methods A **506**, 149 (2003).
18. S.E. Mughabhghab *et al.*, *Neutron Cross Section* (Academic Press, 1984).
19. H.J. Brede *et al.*, Nucl. Instrum. Methods A **274**, 332 (1989).
20. L.P. Ekström, R.B. Firestone, *WWW Table of Radioactive Isotopes*, database version 2/28/99 from URL `http://ie.lbl.gov/toi/index.htm`.
21. L. Maunoury *et al.*, Nucl. Phys. A **701**, 286c (2002).
22. Y. Bourlat, J.-C. Millies-Lacroix, D. Abt, Nucl. Instrum. Methods A **339**, 309 (1994).
23. CNRS-IN2P3/CEA-DSM, Laboratoire Souterrain de Modane, `http://www-lsm.in2p3.fr`.
24. J.-M. Laborie, G. Le Petit, D. Abt, M. Girard, Nucl. Instrum. Methods A **479**, 618 (2002).
25. J.-M. Laborie, G. Le Petit, D. Abt, M. Girard, Appl. Rad. Isot. **53**, 57 (2000).
26. O. Sima (1999) (sold by MATEC GmbH, Germany).
27. O. Sima, D. Arnold, Appl. Radiat. Isot. **53**, 51 (2000).
28. O. Roig *et al.*, Nucl. Instrum. Methods **521**, 5 (2004).
29. F. Bečvář, Nucl. Instrum. Methods A **417**, 434 (1998).
30. `http://www-nds.iaea.org/RIPL-2/`.
31. `http://www.nndc.bnl.gov/ensdf/`.
32. S. Hilaire, private communication.